

MAGNETIC DAMPING OF SOLID SOLUTION SEMICONDUCTOR ALLOYS

Dr. Frank R. Szofran, Principal Investigator
ES75/Space Sciences Laboratory, NASA Marshall Space Flight Center, Huntsville, AL 35812
Phone: 256-544-7777, Fax: 256-544-8762, e-mail: frank.szofran@msfc.nasa.gov

Co-Investigators:

Prof. Dr. K.W. Benz, Dr. Arne Cröll, Dr. Peter Dold
Kristallographisches Institut der Universität, Freiburg, Germany

Dr. Sharon D. Cobb, Dr. Martin P. Volz
ES75, Marshall Space Flight Center, Huntsville, AL

Dr. Shariar Motakef, Dr. L.B. Vujisic[contributor who is not a Co-Investigator]
CAPE Simulations, Inc., Newton, MA

5106-26
08/13

1 Objectives of the Investigation

The objective of this study is to (1) experimentally test the validity of the modeling predictions applicable to the magnetic damping of convective flows in electrically conductive melts as this applies to the bulk growth of solid solution semiconducting materials and (2) assess the effectiveness of steady magnetic fields in reducing the fluid flows occurring in these materials during processing. To achieve the objectives of this investigation, we are carrying out a comprehensive program in the Bridgman and floating-zone configurations using the solid solution alloy system Ge-Si. This alloy system has been studied extensively in environments that have not simultaneously included both low gravity and an applied magnetic field. Also, all compositions have a high electrical conductivity, and the materials parameters permit reasonable growth rates.

An important supporting investigation is determining the role, if any, that thermoelectromagnetic convection (TEMC) plays during growth of these materials in a magnetic field. TEMC has significant implications for the deployment of a Magnetic Damping Furnace in space. This effect will be especially important in solid solutions where the growth interface is, in general, neither isothermal nor isoconcentrational. It could be important in single melting point materials, also, if faceting takes place producing a non-isothermal interface.

2 Microgravity Relevance

During Bridgman or floating zone growth of semiconductors, generation of destabilizing temperature gradients in the melt is unavoidable, resulting in buoyancy-induced convective mixing of the liquid phase. On Earth this convective mixing is generally very intensive and interferes with segregation of melt constituents at the growth front. Crystal growth in low Earth orbit provides the opportunity to reduce the buoyancy-induced convective intensity; in some cases, mass transfer diffusion-controlled growth may be achieved if the residual acceleration direction and magnitude can be controlled. However, calculations and recent flight experiment results clearly indicate that simply reducing the steady-state acceleration to values achievable in low-Earth orbit will not provide diffusion controlled growth conditions for solid solution melts ~1cm in diameter if accelerations transverse to the growth axis are not controlled. Magnetic damping of convection in electrically conductive melts can be used to provide a higher degree of control on convection in the melt. Magnetic damping effects both buoyancy-induced and Marangoni convection and may enable

diffusion controlled growth without the control of the growth direction relative to the residual steady-state acceleration. Thus our understanding of convective influences on melt-growth processes can be further advanced, and our ability to interpret space experimental results may be significantly improved.

3 Results

3.1 Vertical Bridgman Growth

3.1.1 Calculations

The calculations were performed for the entire system including the furnace, the cartridge, and the charge. In this approach, the furnace setpoints were the inputs into the model; the temperature field in the entire system, the growth interface shape, and the melt composition were the model output. Convection in the melt was modeled to be driven by thermo-solutal buoyancy forces, and the growth interface shape was calculated from the phase diagram for Ge-Si. The simulations were conducted iteratively, where at each iteration the growth interface shape was updated.

Temperature, concentration, and velocity fields are obtained as a solution of coupled axisymmetric energy, species, momentum, and mass conservation equations. Buoyancy (thermal and solutal) was incorporated using the Boussinesq approximation. The applied magnetic field was parallel to the gravity vector and the growth direction.

We have assumed that the growth rate is equal to the pull rate of $0.8\mu\text{m/s}$, and that the segregation coefficient is constant and equal to 4.3 (which corresponds to the segregation coefficient at 5 at% Si). The set points used in the calculations resulted in a nearly constant gradient of $\sim 43\text{ }^\circ\text{C/cm}$ in the ampoule wall over the whole melt domain.

Simulation results indicate that in spite of axial solutal stabilization of convection in the melt, the effect of thermo-solutal convection on radial segregation is strong; elimination of this effect requires significant reduction of gravity to 10^{-5} to 10^{-6} levels or application of large magnetic fields close to 6T on Earth.

3.1.2 Experiments

A series of $\text{Ge}_{1-x}\text{Si}_x$ alloys, with nominal silicon concentrations of 5 at %, has been grown by the vertical Bridgman method. A seven-zone furnace was used to obtain a constant axial thermal gradient of 35°K/cm along the length of the ampoule. Such a constant axial gradient can reduce inevitable radial thermal gradients that arise as a result of differences between the thermal conductivity of the solid and liquid phases and the ampoule.¹ In order to assess the effect of ampoule thermal conductivity on interface shapes and radial segregation, alloys were grown in graphite, hot-pressed boron nitride, and pyrolytic boron nitride ampoules for comparison. All the samples reported here were solidified with a furnace translation velocity of $0.4\mu\text{m/s}$. For each crystal growth experiment, a static axial magnetic field of either 0 or 5 Tesla was applied.

The ampoules were loaded with 8-mm diameter Ge and Si ingots, placed on top of Ge seeds, with a $\langle 100 \rangle$ crystallographic orientation. After the ampoules were placed in the furnace, the furnace was lowered until part of the Ge seed was melted. The furnace was held at this position for up to 72 hours to let the melt completely homogenize. During the homogenization time, and prior to translation, crystal growth occurred until the Si concentration in the solid was in equilibrium with the

Si concentration in the melt, such that $C_S = k(C_L)C_L$, where C_S is the Si concentration in the solid, C_L is the Si concentration in the liquid, and k is the segregation coefficient. Initially, the temperature of the solid/liquid interface is the melting point of Ge. Silicon diffuses downwards towards this interface, increasing the Si concentration, and moving the phase boundary upwards with respect to the furnace. This period of regrowth has been previously described.² The furnace was then translated upward until the entire sample had solidified. After growth, the axial and radial concentration profiles were measured by microprobe and energy dispersive x-ray (EDX) spectroscopy. The microstructure was revealed after etching by means of Nomarski Differential Interference Contrast microscopy (NDIC).

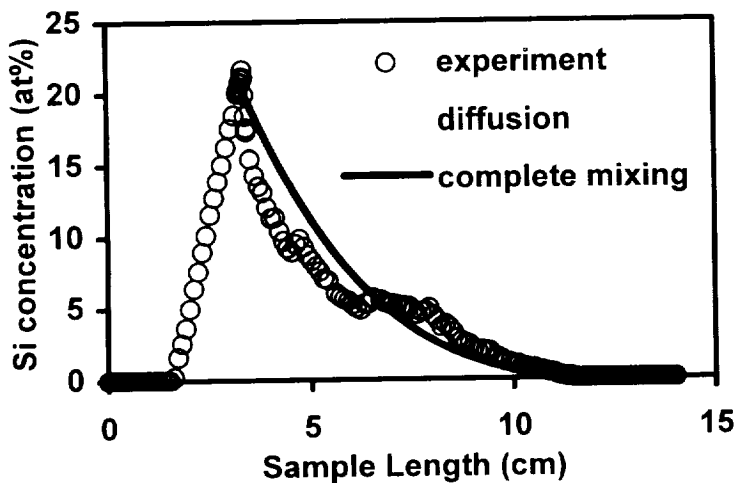


Figure 1. Axial composition profile for a $\text{Ge}_{1-x}\text{Si}_x$ alloy grown in a 5 Tesla axial static magnetic field with a furnace translation rate of $0.4 \mu\text{m/s}$.

Figure 1 shows a typical axial segregation profile. This particular profile was obtained from a sample grown in a hot-pressed boron nitride ampoule and in a 5 Tesla field. In addition to the experimental data, the figure also shows a complete mixing curve, determined from the Pfann relation, and data from a one-dimensional diffusion model. The diffusion model takes into account the variation in segregation coefficient with respect to the liquidus composition. The Ge seed portion of the crystal is that below approximately 2 cm. The steep increase in Si concentration from 0 to 22 at % indicates the period of regrowth. The sudden drop in Si concentration indicates where furnace translation begins. All of the samples, regardless of the ampoule material and whether a 5 T field was applied, exhibit very similar behavior during the initial transient of the axial segregation profile. That is, the experimental data, in the initial transient region, are much better fit by the diffusion model than by the complete mixing model. However, after the initial transient, axial segregation profiles for all of the samples deviate at least somewhat from that expected for diffusion-controlled growth, particularly in the final transient region.

For the same sample, the largest degree of concavity in the radial segregation data is found in the initial transient region, where the change in the axial profile is also the largest. In the data examined to date, no clear distinction was observed between the radial profiles of samples grown with or without an applied field.

With the exception of the sample grown in a graphite ampoule, all samples remained single crystal up to where they reached a maximum Si concentration. The sample grown in a graphite ampoule had a highly concave interface and became polycrystalline even in the regrowth portion of the sample. In general, striations were observed in the regrowth portion of the samples. The samples

remained single crystals for 1-2 mm beyond the point of maximum Si concentration where multiple grains, and in some cases large striations, were observed. An increase in the concavity of the interface shapes was also observed in this region. It is possible that the large change in lattice constant, as a result of a steep drop in Si concentration, is responsible for the deviation from single crystallinity. No clear distinction in the morphology between samples grown with or without a 5 T field was observed.

3.2 Float Zone Growth

The critical Marangoni number for silicon, which describes the transition from laminar to time-dependent flow, has been determined to be ≈ 150 .³ Therefore even small zone geometries result in time dependent Marangoni convection, leading to an irregular microscopic growth velocity and to dopant striations in the grown crystal.³ Whereas the time dependency of the flow causes microscopic inhomogeneities, the time-independent, steady convection effects only the macrosegregation.⁴ In this project, the influence of a static axial magnetic field (variable between $B=0$ and $B=5$ T) on the microsegregation, the macrosegregation, and the interface curvature has been analyzed. Except to note that magnetic fields tend to flatten the interface, this report will discuss only the segregation results.

3.2.1 Experimental setup and growth technique

The growth experiments were performed in a monoellipsoid mirror furnace.⁵ The 8 mm diameter samples were mounted wall-free and sealed in the ampoules with argon or oxygen. B, Ga, P, As, and Sb were used as dopants. Zone heights in the range of 8 to 12 mm were established. Calculations of the temperature field have been performed,^{6,7} which predict axial temperature gradients of ≈ 100 -150 K/cm at the solid/liquid interface and a maximum temperature difference of ≈ 30 -50 K between the interface and the half of the zone height (temperature maximum) for the case of diffusive heat transport. These values will be reduced by convection. The usual translation rate was 4 mm/min. The maximum grown length was approximately 40 mm. The furnace was positioned in the center of a superconducting solenoid. The floating zone was monitored by a borescope and a CCD-camera.

3.2.2 Preparation and characterization of the grown crystals

The grown crystals were cut lengthwise along the (110)-plane, polished, etched using the WRIGHT etch,⁸ and analyzed qualitatively by NDIC (Nomarski Differential Interference Contrast Microscopy). Four-point probe and spreading resistance measurements were carried out on selected samples.

3.2.3 Results

The axial macroscopic segregation is shifted towards a more diffusion-controlled profile with higher induction. However, experiments with pill doping and oxide coated samples⁹ show that even at 5 Tesla diffusion-controlled growth has not been obtained. This result is corroborated by numerical simulations.¹⁰

In contrast to the macrosegregation results, the magnetic field has a substantial influence on the microsegregation of the grown crystals: Crystals grown without magnetic field have strong and irregular striation patterns caused by time dependent Marangoni convection. These patterns, based on their shape and demarcation experiments, indicate the shape of the growth interface. These striations are eliminated in crystals grown in magnetic fields as low as 500 mT. Unfortunately,

striation-free growth in strong axial fields is not easily reproducible, as a lot of the grown crystals (mostly the As- and Sb-doped samples) showed the unexpected appearance of striations after an initial striation-free area. The striations are never present at the start of growth. They form only after some material is crystallized; stopping the translation and then starting again repeats this sequence. Figure 2 shows an example of these structures. These striations can be quite pronounced and are often of clearly oscillatory nature (note that all the crystals were grown without rotation), in contrast to striations caused by thermocapillary convection. The strength, frequency, and position of these striations varies somewhat between experiments, or even within the same crystal. The frequency range is between 0.1Hz and 10Hz. In contrast to the residual striations detectable outside the core in the case of 100-500mT,^{11,12} they are not limited to the crystal periphery. They do occur in magnetic field grown crystals coated with SiO₂ to suppress thermocapillary convection. The position of these striations often suggests a convectively mixed torus in the zone. They do not always follow the interface shape closely. Several possibilities for the origin of these effects have been considered. The most convincing explanation is thermoelectromagnetic convection (TEMC). TEMC is caused by the interaction of magnetic fields with thermoelectric currents.¹³ The motion in the melt is caused by the Lorentz force resulting from the interaction of the thermoelectric current with the magnetic field. For materials with good conductivity and high thermoelectric coefficients, these currents can reach considerable values and TEMC can be the dominant source of convection. The gradient of the thermovoltage, the source of the current, may be due to temperature gradients, the difference in the Seebeck coefficient between liquid and solid, or possibly also by changes of the Seebeck coefficient due to compositional inhomogeneities. Strong effects should be expected if facets are present, due to the undercooling of the liquid in front of the facet interface. As only the current components perpendicular to the field lines lead to a Lorentz force, the TEMC in axial fields is mainly driven by radial gradients, which in turn leads to an azimuthal flow. The field also damps convection due to TEMC, so the azimuthal velocity goes through a maximum as a function of the induction.

The application of strong axial magnetic fields is an interesting tool for controlling the segregation in silicon floating zones, but one that has to be used with caution. The axial macrosegregation, usually close to the complete mixing case due to strong thermocapillary convection, can be shifted towards a

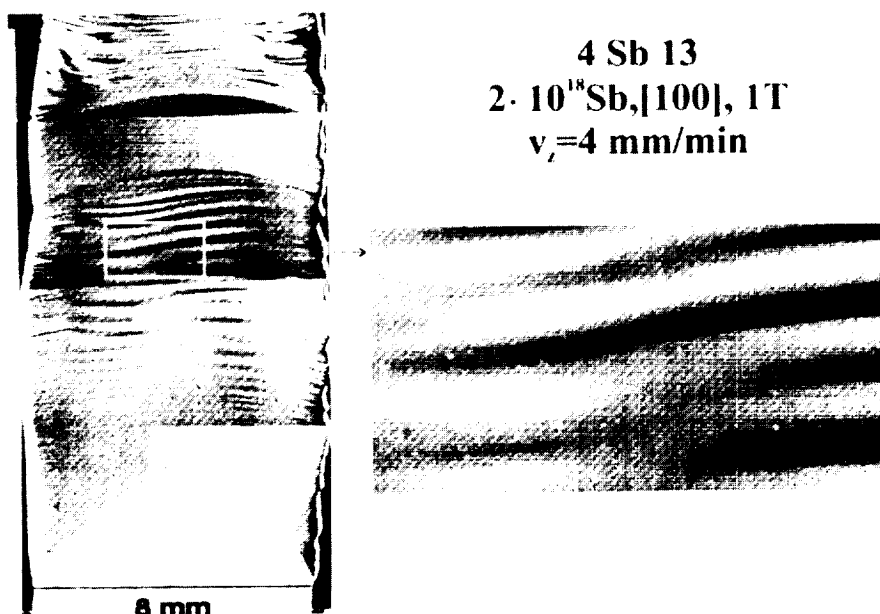


Figure 2. Silicon float-zone sample showing initial absence of striations followed by the appearance of TEMC-induced striations.

more diffusion-controlled regime, but it is not possible to attain purely diffusive conditions even with fields of 5T. This is only possible by the combination of microgravity and a coated melt surface.⁹ The radial segregation is initially deteriorated by the application of axial fields < 1T due to the separation of the flow field into two areas, a quiescent center and a thin boundary layer strongly mixed by thermocapillary convection.^{11,14} The thickness of the outer layer, however, is dependent on induction, and fields $\geq 1T$ are sufficient to reduce it to insignificant values.

Strong fields suppress time-dependent thermocapillary convection completely, thus eliminating the striations associated with it. However, a new type of striations was found in some of the crystals. The striations, often exhibiting strong periodicity, usually do not appear at the outset of growth, but only after some material has been grown. The explanation consistent with the experimental results is that they are caused by thermoelectromagnetic convection, originating from the interaction of thermoelectric currents with the field. A radially oriented current in an axial magnetic field leads to an azimuthal flow. In the case of axial fields, a deviation from circular symmetry (of the isotherms, the crystal position, due to faceting etc.) is necessary to generate a net current. This explains the fact that the effect is not always observed.

4 Summary

Magnetic fields up to 5 Tesla are sufficient to eliminate time-dependent convection in silicon floating zones and possibly Bridgman growth of Ge-Si alloys. In both cases, steady convection appears to be more significant for mass transport than diffusion, even at 5 Tesla in the geometries used here. These results are corroborated in both growth configurations by calculations.

¹ A. Rouzaud, D. Camel and J. J. Favier, *J. Crystal Growth* 73 (1985) 149-166.

² L. Helmers, J. Schilz, G. Bahr, and W. A. Kaysser, *J. Crystal Growth* 154 (1995) 60-67.

³ A. Cröll, W. Müller-Sebert, K. W. Benz and R. Nitsche: *Microgravity sci. technol.* III/4 (1991) 204.

⁴ W. A. Tiller, K. A. Jackson, J. W. Rutter and B. Chalmers: *Acta Met.* 1 (1953) 428.

⁵ A. Eyer, H. Leiste and R. Nitsche: *J. Crystal Growth* 71 (1985) 173.

⁶ P. Dold, PhD-Thesis, University of Freiburg, Germany (1994).

⁷ D. Langbein and H. J. Sattler, *BMFT-Report BleV-R-65.424-4* (1984).

⁸ M. Wright Jenkins: *J. Electrochem. Soc.* 124,5 (1977) 757.

⁹ A. Cröll, W. Müller and R. Nitsche: *J. Crystal Growth* 79 (1986) 65

¹⁰ Th. Kaiser and K. W. Benz: Submitted to *J. Crystal Growth*

¹¹ A. Cröll, P. Dold and K. W. Benz: *J. Crystal Growth* 137 (1994) 95

¹² P. Dold, A. Cröll, and K. W. Benz: Submitted to *J. Crystal Growth*

¹³ J. A. Shercliff: *J. Fluid. Mech.* 91/2 (1979) 231

¹⁴ P. Dold, A. Cröll, and K. W. Benz: Submitted to *J. Crystal Growth*, Th. Kaiser and K. W. Benz: Submitted to *J. Crystal Growth*, T. E. Morthland and J. S. Walker: *J. Crystal Growth* 158 (1996) 471, C. W. Lan: *J. Crystal Growth* 169 (1996) 269